Extinction efficiencies of mixed aerosols measured by aerosol cavity ring down spectrometry

WANG Lei[1,2], WANG WeiGang[1] & GE MaoFa[2*]

[1] State Key Laboratory for Structural Chemistry of Unstable and Stable Species, Beijing National Laboratory for Molecular Sciences, Institute of Chemistry, Chinese Academy of Sciences, Beijing 100190, China;

[2] Beijing National Laboratory for Molecular Science, State Key Laboratory for Structural Chemistry of Unstable and Stable Species, Peking University, Beijing 100871, China

A cavity ring down spectroscopy instrument was introduced and designed for measuring extinction efficiencies of pure and mixing aerosols in this paper. Through averaging 500 individual waveforms, the minimal detectable aerosol extinction coefficient of 8.4×10^{-7} m^{-1} was achieved. By the test results using the NaCl particles, we concluded that this system could measure the extinction efficiencies of an aerosol with an uncertainty less than 3% under laboratory controlled experimental conditions. The refractive indices of different aerosols were retrieved through comparing the measured extinction efficiencies of each aerosol type with which predicted by Mie theory. Aerosols composed of ammonium sulphate and succinic acid with different weight ratios were used to create a model of mixed aerosols using these two materials, whose extinction efficiencies and complex refractive indices were derived. The refractive indices of the mixed aerosols were also calculated by various optical mixing rules. We found that all the molar refraction/absorption mixing rule, the volume ratio linear rule, and Maxwell-Garnett rule did provide comparable results, of which the volume ratio linear rule gave a slightly worse fit than the others.

cavity ring down spectroscopy, optical property, mixing aerosols, mixing rules

Aerosol particles could largely affect the radiative balance of the atmosphere, which is mainly determined by the optical properties dependent on the sizes, morphology, and complex refractive indices of aerosols. Unlike long-lived greenhouse gases such as CO_2 and CH_4, whose radiative forcing (RF) values measured by high precision ($+2.63\pm0.26$ W m^{-2}), the effects of aerosols on the radiation are still poorly quantified. According to the Fourth Assessment of the Intergovernmental Panel on Climate Change [1,2], total direct aerosol RF amounts to -0.5 ± 0.4 W m^{-2}, with a low level of scientific explanation. The wide range of radiative forcing suggests that there remains a significant uncertainty which limits our ability to quantify the effect of human emissions on climate. Therefore, to explore accurate measurements of aerosol scattering and absorption is crucial for estimating the Earth's energy balance. Compared with scattering light, the photons absorbed will disappear and cannot be detected easily. Also to measure the absorption has also been proven to be more difficult than to measure scattering. Two traditional measurements of absorption, the Particle Soot Absorption Photometer (PSAP) and Aethalometer, measure the light reflected from or transmitted through a particle-laden filter [3,4]. Due to the multiple scattering caused by the particle aggregate and filter, most atmospheric aerosol absorption and scattering data based on these measurements come with bias in the range of 20%–35% [4,5] and 30%–35% [6,7] respectively. For these filter-based techniques, some correction factors are necessary. Recently, photoacoustic spectroscopy has been used to measure the absorption of laboratory and atmospheric aerosol particles [8−10]. In this tech-

*Corresponding author (email: gemaofa@iccas.ac.cn)

nique, the variation of temperature in the sample cell could result in an acoustic signal, which can be detected with a microphone. This technique provides a method for rapidly, real-time measuring the absorption, yet the interference still exists because heat and mass transfers when volatile species evaporate due to heat, especially under high relative humidity (RH) conditions [9,11]. The cavity ring down spectroscopy system was first developed in 1988 by O'Keefe and Deacon [12]. In recent years, the implementation of cavity ring down spectroscopy (CRDS) to measure extinction properties has become popular thanks to its high sensitivity and ability to measure the absolute extinction of an aerosol sample. As a direct absorption measurement technique, the CRDS has many advantages over traditional techniques. Firstly, this technique belongs to a category of absolute methods, which can measure the extinction of aerosols without instrument calibration. Besides, CRDS is also largely immune to the laser intensity, and could contribute to a long effective path length in extinction. Due to these merits above, it has become a widely used new tool for measurement of gaseous trace species in the troposphere [13,14], kinetic studies [15–17], and extinction coefficients of laboratory and ambient aerosols [18–27].

In this study, a cavity ring down spectroscopy (CRDS) was designed for determining the extinction efficiency and complex refractive indices of pure and mixed aerosols. To test its performance, this new setup is applied on the optical properties of sodium chloride with well known indices of refraction. Then we determined the Q_{ext} of ammonium sulphate and succnic acid as pure component aerosols and mixing aerosols and used Mie scattering calculations to retrieve their refractive indices. The results allow us to test the reliability of this system and the appropriateness of the different mixing rules.

1 Experimental

1.1 Aerosol generation and classification

Aerosols were generated by nebulizing solution using a constant output atomizer (Model 3072, TSI Inc.) with dry particle-free zero air (Model 111, Thermo Scientific). The particles are dried by a silica diffusion dryer and a PD-50T-12ss (RH<5%), yielding a polydisperse aerosol distribution. The dry aerosol passed through a neutralizer to obtain an equilibrium charge distribution and then through a differential mobility analyzer (DMA, Model 1500, MSP) to select a selected particle size. The size-selected monodisperse aerosol flow was directed into the CRDS for extinction coefficient measurement. A condensation particle counter (CPC, Model 3772, TSI Inc.) was connected to the outlet of the CRDS to measure particle number concentration.

1.2 Cavity ring down spectroscopy (CRDS) system

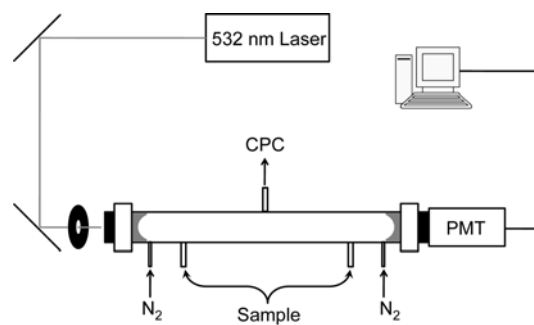The schematic diagram of the CRDS is shown in Figure 1.

Figure 1 Schematic diagram of the cavity ring down spectroscopy system.

Briefly, it consists of two highly reflective concave mirrors (curvature radii of 6 m and a reflectively of 99.995% at 532 nm, Los Gatos, USA) and a stainless steel cell. The mirrors are mounted at the two sides of a 87 cm, 2 cm i.d. stainless steel tube. A Nd-TAG laser system (10 Hz, 3–5 ns, New Wave™ Research, Inc.) is used to generate light pulses at 532 nm that are introduced into the cavity to monitor the optical properties of aerosols. The intensity of the light exiting the cavity, $I(t)$ is measured by a photomultiplier located at one end of the cavity. A small purge flow of dry particle-free nitrogen 0.03 SLM is introduced in front of each mirror to prevent mirror contamination by deposition of aerosols.

The aerosol flow enters the CRDS cell through two tubes on the left and right of CRDS cell. The flow is 0.5 L/min in both lines and the total flow inside the cavity is 1.0 L/min. The particle flow exit the cavity from tube in the middle of the CRDS cell and their concentration is determined by a CPC. The length of the cavity occupied by particles during the flow is about 0.72 m. To ensure that the particle losses are negligible, the particle number density is measured after the DMA and at the end at the exit of the CRD cell. In both cases, the particle number density was almost identical (>97%), for all particles sizes, suggesting minimal loses in the CRDS system. The performance of the CRDS system was checked with several different sizes of sodium chloride (NaCl).

Because the amount of light transmitted through the mirror is proportional to the amount of light still trapped inside the cavity. In the case of a cavity free of scattering or absorption particles, the light intensity within the cavity will decrease exponentially according to the following relationship:

$$I(t) = I_0 \exp\left[-(1-R)\frac{tc}{L}\right], \qquad (1)$$

where I_0 is the initial light intensity, $I(t)$ is the light intensity after t, c is the velocity of light, R is the reflectivity of the mirrors, and L is length of the cavity (distance between the two mirrors). When the cavity is filled with an absorption or scattering medium, the total loss in the cavity will be given by

$$I(t) = I_0 \exp\left\{-\left[(1-R)+\alpha_{ext}l\right]\frac{tc}{L}\right\}. \qquad (2)$$

From which the time constant τ for the decay will be given by

$$\tau = \frac{L}{c[(1-R)+\alpha_{ext}l]}, \qquad (3)$$

where α_{ext} is the extinction coefficient of the molecules or particles inside the cavity, and l is actual distance in the cavity filled with sample. The extinction coefficient α_{ext} can be given directly through the expression:

$$\alpha_{ext} = \frac{L}{cl}\left(\frac{1}{\tau}-\frac{1}{\tau_0}\right). \qquad (4)$$

The α_{ext} of homogeneous spheres (aerosol) is described by

$$\alpha_{ext} = N\sigma_{ext} = \frac{1}{4}N\pi D^2 Q_{ext}, \qquad (5)$$

where σ_{ext} is the extinction cross section, Q_{ext} is the extinction efficiency of the particles which is the ratio of Beer's law extinction cross section to the geometric area of the particle and its dimensionless.

The light leaking out of the cavity through one of the mirror is detected with a photomultiplier (Hamamatsu CR131) and the resulting signal is fed into digitized storage oscilloscope (Tektronix, Model DPO 2024, 200 MHz), which is triggered simultaneously with the laser pulse. The data is transferred and stored in a personal computer using a Lab-VIEW program. To detrimental the minimum detectable extinction coefficient the following definition for the detection limit [26]:

$$\alpha_{min} = \frac{L}{C \times d}\frac{\Delta\tau_{min}}{\tau_0^2}, \qquad (6)$$

where $\Delta\tau_{min}$ is the standard deviation of the decay time for 500 shots which was obtained for a cavity filled with only zero air. In the experiment presented here, $\tau_0 = 12$ μs (τ_0 is the decay time for cavity filled only with zero air) and $\Delta\tau_{min} = 0.03$ μs for an average of a 500 laser shots operating 10Hz. This results produced the minimum detectable extinction coefficient of 8.4×10^{-7} m^{-1}.

2   Results and discussion

2.1   Tested by NaCl particles

The optical properties of NaCl are well known in the literature [28,29]. Therefore, we measured the optical properties of NaCl with well known indices of refraction to test the CRDS. The extinction coefficients as a function of the particles concentration of NaCl at different size were measured.

As shown in Figure 2, the extinction coefficients increased linearly with particle concentration and the particles extinction cross-section (σ_{ext}) is determined by using the eq. (5). Therefore, the σ_{ext} is the slope of the linear fit for each size in Figure 2. At the meanwhile, the extinction efficiency (Q_{ext}) is also can calculated by eq. (5). By comparing the measured extinction efficiency with the extinction efficiency calculated using Mie scattering theory for homogeneous spheres, the particle refractive index is obtained by minimizing the merit (χ) function:

$$\chi^2(n,k) = \sum_{i=1}^{N}\frac{(Q_{ext,measured}-Q_{ext,calculated}(n,k))_i^2}{\varepsilon_i^2}, \qquad (7)$$

where n and k denote the real and imaginary parts of the refractive index, respectively.

For every particle size, the measurement is performed subsequently with several different particles concentrations, so that ε_i, the measurement error for particle size i, given by the standard deviation of the individual extinction efficiencies, is also determined. Figure 3 illustrate the extinction efficiencies of NaCl as a function of size parameter x ($x = \pi D/\lambda$). The points are obtained by the CRDS measurement
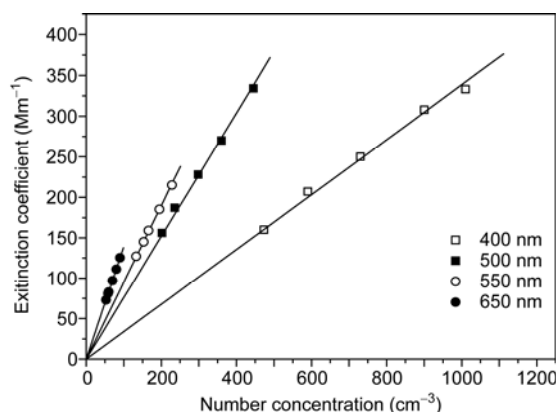

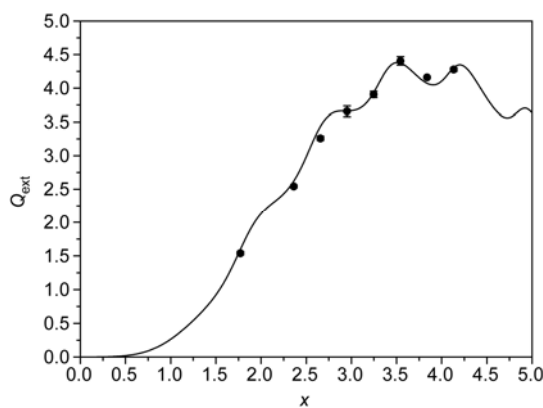**Figure 2**   Extinction coefficient at 532 nm measured as a function of particles number concentrations of NaCl.

Figure 3   The extinction efficiency (Q_{ext}) as a function size parameter (x) of NaCl.

for different sizes of NaCl and curves are obtained from Mie fit using refractive index of 1.546+0.003i [28,29]. We also use the data measured by CRDS to calculated refractive index using Mie theory, yielding a refractive index of 1.536+0.000i for NaCl, which agree well with the published results [28].

2.2 Homogeneously internally mixed aerosols

A number of methods for calculating the radiative properties of aerosols of mixed composition are used in climate models. In this study, three mixing rules currently are used: (1) a volume-weighted linear average of the refractive indices [30]; (2) molar refraction and absorption [31,32]; (3) the Maxwell-Garnett rule [33].

The "linear mixing rule" assumes that the total real and imaginary refractive indices of the mixture are given linear average of the indices of the components by their volume fractions:

$$n_{\mathrm{tot}} = f_1 n_1 + f_2 n_2, \tag{8}$$

$$k_{\mathrm{tot}} = f_1 k_1 + f_2 k_2, \tag{9}$$

where f_i is the volume fraction of the components.

The molar refraction and absorption mixing rule assumes that the total molar refraction of a mixture is given by the linear average of the molar refraction of the components in the mixture weighted by their molar volumes:

$$R_{\mathrm{tot}} = V_{\mathrm{tot}} \frac{n_{\mathrm{tot}}^2 - 1}{n_{\mathrm{tot}}^2 + 1} = \chi_1 R_1 + \chi_2 R_2, \tag{10}$$

$$A_{\mathrm{tot}} = V_{\mathrm{tot}} k_{\mathrm{tot}} = \chi_1 A_1 + \chi_2 A_2, \tag{11}$$

where R_{tot}, V_{tot}, n_{tot}, A_{tot} and k_{tot} are the molar refraction, molar volume, real part of the refractive index, molar absorption, and imaginary part of the refractive index of the mixture, respectively, and χ_i, R_i, A_i are the molar fraction, molar refraction, and molar absorption of the components, respectively. The molar refraction of the components, molar absorption of the components, and total molar volume are given by

$$R_i = \frac{M_i}{\rho_i} \frac{n_i^2 - 1}{n_i^2 + 2}, \tag{12}$$

$$A_i = \frac{M_i}{\rho_i} k_i, \tag{13}$$

$$V_{\mathrm{tot}} = \frac{M_{\mathrm{tot}}}{\rho_{\mathrm{tot}}} = \chi_1 \frac{M_1}{\rho_1} + \chi_2 \frac{M_2}{\rho_2}, \tag{14}$$

where M symbolizes molecular weight, and ρ symbolizes density.

In the Maxwell-Garnett mixing rule, one or more of the components are deemed "inclusions", while the rest of the components comprise a "homogeneous matrix". The inclusions are assumed to be small, spherical, randomly distributed throughout the drop, such that the effective dielectric constant of the mixture is given by

$$\varepsilon_{\mathrm{tot}} = \varepsilon_{\mathrm{matrix}} + \frac{3 f_{\mathrm{incl}} \varepsilon_{\mathrm{matrix}} (\varepsilon_{\mathrm{incl}} - \varepsilon_{\mathrm{matrix}})}{\varepsilon_{\mathrm{incl}} + 2\varepsilon_{\mathrm{matrix}} - f_{\mathrm{incl}} (\varepsilon_{\mathrm{incl}} - \varepsilon_{\mathrm{matrix}})}, \tag{15}$$

$$n_{\mathrm{tot}} = (\varepsilon_{\mathrm{tot}})^{1/2}, \tag{16}$$

where $\varepsilon_{\mathrm{tot}}$, $\varepsilon_{\mathrm{incl}}$, and $\varepsilon_{\mathrm{matrix}}$ are the complex dielectric constants of the mixture, the inclusions, and the matrix, respectively, f_{incl} is the volume fraction of the inclusions and n_{tot} is the complex refractive index of the mixture.

Aerosols in atmospheric are more complex than laboratory generated pure aerosols. Typically they are composed of mixtures of inorganic and organic molecules that can be arranged in different ways, such as homogeneous mixtures or as coated particles. Urban and pollution aerosols contain both organic and inorganic components [34]. Therefore, exploring the optical properties of mixed particles is important for the exploring the optical properties of atmospheric aerosols. To do so, we studied the optical properties of mixed $(NH_4)_2SO_4$ and succinic acid (SA) particles, which are common components of urban particles. First we measured the optical properties of pure $(NH_4)_2SO_4$ and SA aerosols. Then we measured the optical properties of the mixture of these two components prepared with different known weight ratios (1:2, 1:1, 2:1). We assumed that the aerosols generated from these solutions are homogeneous and that the weight ratio of the solution is maintained in the aerosols, because both compounds dissolve very well in water. The assumption is later verified by calculations of the refractive index. The extinction efficiency as a function of size parameter for particles of $(NH_4)_2SO_4$, SA, and the particles generated from the mixture with weight ratios of $(NH_4)_2SO_4$ and SA of 1:1, 1:1 and 2:1, respectively, are shown in Figure 4.

The Q_{ext} of laboratory-generated aerosols comprised of internal mixtures of $(NH_4)_2SO_4$ and succinic acid (SA) with weight ratio of 1:2, 1:1 and 2:1 was measured with CRDS. The aerosol refractive index retrieval was then used to test which mixing rule provides the best match to the measurements. Because the imaginary refractive indices of these compounds were zero at 532 nm, we would refer to refractive indices and the real part of the refractive indices interchangeably below. Using the CRDS, the RI of the pure constituents that made up the mixture were retrieved (RI=1.530 for pure $(NH_4)_2SO_4$ and RI=1.450 for pure succinic acid). The experiment data were determined using the merit function (eq. (7)).

2.3 Calculations using mixing rules

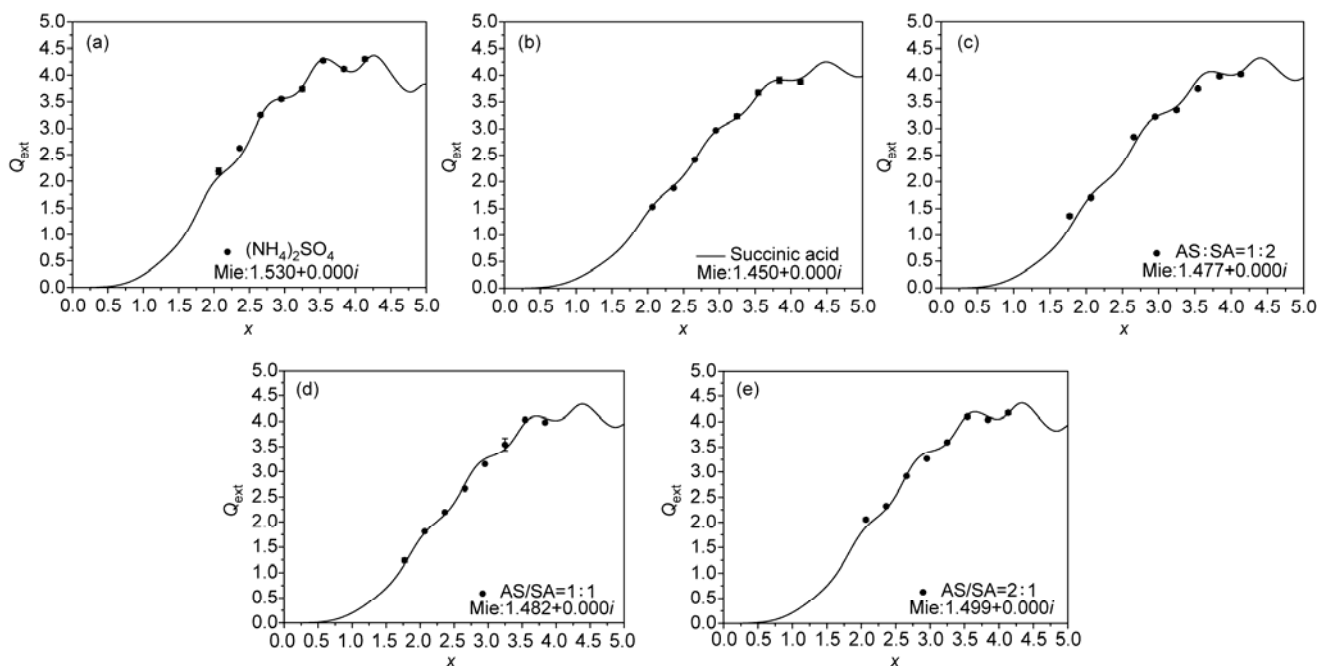As stated above, optical properties of aerosols in the

Figure 4   Extinction efficiency (Q_{ext}) as a function of size parameter (x) obtain for ammonium sulfate, succinic acid, and the mixtures of $(NH_4)_2SO_4$ (a) and succinic acid (b) with weight ratio of AS/SA: 1:2 (c), 1:1 (d), and 2:1 (e), respectively. The solid curves are the result of the Mie fit to the experimental points.

atmosphere are often calculated using various mixing rules and models. However, it is often impossible to verify the validity of these calculations. Using this system, it is possible to generate particles of known composition and structure and to retrieve the refractive index, which can be compared to calculations by different mixing rules.

We employ a variety of mixing rules to calculate the complex index of refraction for mixed aerosol and compare the calculated index with the index retrieved from our measurements. The refractive indices retrieved for pure $(NH_4)_2SO_4$ and SA aerosols are used as input for calculating the refractive indices of the mixture by different mixing rules. In all cases, $(NH_4)_2SO_4$ is treated as the matrix and SA as the inclusion.

Results of these calculation for 1:2, 1:1, and 2:1 mixtures of $(NH_4)_2SO_4$ and SA are given in Table 1. The calculations are done for all the size. Mixing rules (1) and (2) result in good agreement with the measurements. The best fit mixing rule is obtained with the molar refraction and absorption rule and Maxwell-Garnett, although the volume linear rule also provide a slightly worse fit for the values measured and may also be appropriate for use in the models. The core plus shell model also produced a higher error than mixing rules (1)–(3), as might be expected from the fact that the $(NH_4)_2SO_4$ and SA are homogeneously mixed in solution, not layered.

The refractive indices obtained by using mixing rules are very close to those retrieved from experiments data for mixtures. For example, molar refraction and absorption rule

Table 1   The index of refractive of $(NH_4)_2SO_4$, succinic acid, and their mixture obtained by different mixing rules

Sample	RI retrieved	RI calculated by different mixing rules		
		(1)	(2)	(3)
$(NH_4)_2SO_4$	1.530	–	–	–
Succinic acid	1.450	–	–	–
1:2 (AS:SA)	1.477	1.474	1.475	1.474
1:1 (AS:SA)	1.482	1.487	1.488	1.487
2:1 (AS:SA)	1.499	1.501	1.501	1.501
$s=\sqrt{\sum\left(RI_{cal}-RI_{retrieved}\right)^2}$	–	6.2×10^{-3}	6.7×10^{-3}	6.2×10^{-3}

for all the sizes of the mixture ($(NH_4)_2SO_4$:SA=1:2) produce a refractive index of $n=1.474$, while retrieved refractive index is $n=1.477$. A comparison between the extinction efficiency as a function of the size parameter of these two refractive indices and the residual between the curves are shown in Figure 5. The curves are so close that the differences appear at all size parameters could be negligible.

3   Conclusions

We established a CRDS to provide a sensitive determination of an aerosol extinction coefficient in real time. The result of NaCl particles tested showed that CRDS could measure
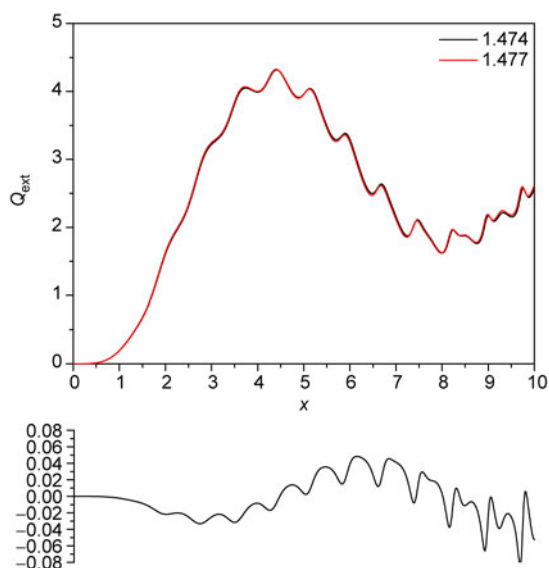
Figure 5 Comparison between the refractive index obtained using molar refractive and absorption mixing rule for the mixture ((NH$_4$)$_2$SO$_4$: SA=1 : 2, n=1.474) and the refractive index retrieved from measurements of the same mixture using Mie theory (n=1.477).

the aerosol extinction coefficient with an uncertainty 3% under laboratory controlled experimental conditions. The refractive indices for these aerosols were retrieved from the measurements using Mie theory and agree with data in the literature. Among the different mixing rules, the molar refraction and absorption and Maxwell-Garnett rule provided the best fit, suggesting that for the non-absorbing species, these rules would be the best to predict the index of refraction. Volume linear mixing rule also gave very good agreement with the measured values, only with a little slightly worse fit than the former two.

1   Solomon S, Qin D, Manning M, et al. In: Climate Change 2007: The Physical Science Basis. Contribution of Working Group I to the Fourth Assessment Report of the Intergovernmental Panel on Climate Change. UK and New York: Cambridge University Press, 2007

2   Rachael E H, Miles S R, Andrew J, et al. Sources of error and uncertainty in the use of cavity ring down spectroscopy to measure aerosol optical properties. Aerosol Sci Technol, 2011, 45: 1360–1375

3   Sheridan P J, Arnott W P, Ogren J A, et al. The reno aerosol optics study: An evaluation of aerosol absorption measurement methods. Aerosol Sci Technol, 2005, 39: 1–16

4   Bond T C, Anderson T L, Campbell D. Calibration and intercomparison of filter-based measurements of visible light absorption by aerosols. Aerosol Sci Technol, 1999, 30: 582–600

5   Magi B I, Hobbs P V, Schmid B, et al. Vertical profiles of light scattering, light absorption, and single scattering albedo during the dry, biomass burning season in southern Africa and comparisons of *in situ* and remote sensing measurements of aerosol optical depths. J

Geophys Res, 2003, 108: doi: 10.1029/2002JD002361

6   Schmid O, Artaxo P, Arnott W P, et al. Spectral light absorption by ambient aerosols influenced by biomass burning in the Amazon Basin. I: Comparison and field calibration of absorption measurement techniques. Atmos Chem and Phys, 2006, 6: 3443–3462

7   Weingartner E, Saathoff H, Schnaiter M, et al. Absorption of light by soot particles: Determination of the absorption coefficient by means of aethalometers. J Aerosol Sci, 2003, 34: 1445–1463

8   Arnott W P, Moosmuller H, Rogers C F, et al. Photoacoustic spectrometer for measuring light absorption by aerosol: Instrument description. Atmos Environ, 1999, 33: 2845–2852

9   Arnott W P, Moosmuller H, Sheridan P J, et al. Photoacoustic and filter-based ambient aerosol light absorption measurements: Instrument comparisons and the role of relative humidity. J Geophys Res, 2003, 108: doi: 10.1029/2002JD002165

10   Cappa C D, Lack D A, Burkholder J B, et al. Bias in filter-based aerosol light absorption measurements due to organic aerosol loading: Evidence from laboratory measurements. Aerosol Sci Technol, 2008, 42: 1022–1032

11   Raspet R, Slaton W V, Arnott W P, et al. Evaporation-condensation effects on resonant photoacoustics of volatile aerosols. J Atmos Ocean Technol, 2003, 20: 685–695

12   O'keefe A, Deacon D A G. Cavity ring-down optical spectrometer for absorption-measurements using laser sources. Rev Sci Instrum, 1988, 59: 2544–2551

13   Mercier M X, Therssen E, Pauwels J F, et al. Quantitative features and sensitivity of cavity ring-down measurements of species concentrations in flames. Combust Flame, 2001, 124: 656–667

14   Schocker A, Kohse-Hoinghaus K, Brockhinke A. Quantitative determination of combustion intermediates with cavity ring-down spectroscopy: Systematic study in propene flames near the soot-formation limit. Appl Optics, 2005, 44: 6660–6672

15   Choi Y M, Park J, Lin M C. Experimental and computational studies of the kinetics and mechanisms for C_6H_5 reactions with acetone-h(6) and -d(6). J Phys Chem A, 2003, 107: 7755–7761

16   Czyzewski A, Ernst K, Franssen G, et al. Investigation of kinetics of CH-radicals decay by cavity ring-down spectroscopy. Chem Phys Lett, 2002, 357: 477–482

17   Nizamov B, Dagdigian P J. Spectroscopic and kinetic investigation of methylene amidogen by cavity ring-down spectroscopy. J Phys Chem A, 2003, 107: 2256–2263

18   Adler G, Riziq A A, Erlick C, et al. Effect of intrinsic organic carbon on the optical properties of fresh diesel soot. Proc Natl Acad Sci USA, 2010, 107: 6699–6704

19   Dial K D, Hiemstra S, Thompson J E. Simultaneous measurement of optical scattering and extinction on dispersed serosol samples. Anal Chem, 2010, 82: 7885–7896

20   Freedman M A, Hasenkopf C A, Beaver M R, et al. Optical properties of internally mixed aerosol particles composed of dicarboxylic acids and ammonium sulfate. J Phys Chem A, 2009, 113: 13584–13592

21   Lang-Yona N, Abo-Riziq A, Erlick C, et al. Interaction of internally mixed aerosols with light. Phys Chem Chem Phys, 2010, 12: 21–31

22   Li L, Chen J, Chen H, et al. Monitoring optical properties of aerosols with cavity ring-down spectroscopy. J Aerosol Sci, 2011, 42: 277–284

23   Mellon D, King S J, Kim J, et al. Measurements of extinction by aerosol particles in the near-Infrared using continuous wave cavity ring-down spectroscopy. J Phys Chem A, 2011, 115: 774–783

24   Miles R E H, Rudic S, Orr-Ewing A J, et al. Measurements of the wavelength dependent extinction of aerosols by cavity ring down spectroscopy. Phys Chem Chem Phys, 2010, 12: 3914–3920

25   Trainic M, Riziq A A, Lavi A, et al. The optical, physical and chemical properties of the products of glyoxal uptake on ammonium sulfate seed aerosols. Atmos Chem Phys, 2011, 11: 9697–9707

26   Xue H, Khalizov A F, Wang L, et al. Effects of dicarboxylic acid coating on the optical properties of soot. Phys Chem Chem Phys, 2009, 11: 7869–7875

27   Brown S S, Stark H, Ciciora S J, et al. Simultaneous in situ detection of atmospheric NO$_3$ and N$_2$O$_5$ via cavity ring-down spectroscopy.

Rev Sci Instrum, 2002, 73: 3291–3301

28   Riziq A A, Erlick C, Dinar E, et al. Optical properties of absorbing and non-absorbing aerosols retrieved by cavity ring down (CRD) spectroscopy. Atmos Chem Phys, 2007, 7: 1523–1536

29   Dinar E, Riziq A A, Spindler C, et al. The complex refractive index of atmospheric and model humic-like substances (HULIS) retrieved by a cavity ring down aerosol spectrometer (CRD-AS). Faraday Discuss, 2008, 137: 279–295

30   d'Almeida G A, Koepke P, Shettle E P, et al. Atmospheric Aerosols Global Climatology and Radiative Characteristics. Hampton: A. Deepak Publishing, 1991

31   Jacobson M Z. Analysis of aerosol interactions with numerical techniques for solving coagulation, nucleation, condensation, dissolution, and reversible chemistry among multiple size distributions. J Geophys Res, 2002, 107: doi: 10.1029/2001JD002044

32   Tang I N. Thermodynamic and optical properties of mixed-salt aerosols of atmospheric importance. J Geophys Res, 1997, 102: 1883–1893

33   Bohren C F, Huffman D R. Absorption and Scattering of Light by Small Particles. New York: Wiley-VCH, 1983

34   Murphy D M, Cziczo D J, Froyd K D, et al. Single-particle mass spectrometry of tropospheric aerosol particles. J Geophys Res, 2006, 111: doi: 10.1029/2006JD007340